Probability Table Monte Carlo Method Applied to CANDU-6 Cell Calculation in DRAGON

N. Martin and A. Hébert
Institut de Génie Nucléaire, École Polytechnique de Montréal
C.P. 6079, succ. Centre-Ville, Montréal, Qc, Canada H3C 3A7

Abstract

We present recent progresses done regarding the development of a Monte Carlo module in the lattice code DRAGON. We propose using probability table cross sections in a Monte Carlo algorithm, as first introduced by D.E. Cullen at LLNL in the Monte Carlo transport code TART. In our case, the CALENDF formalism has been chosen for computing the probability tables, in addition with optimized energy meshes comprising only 295 or 361 groups. An evaluation of the coolant void reactivity (CVR) of a legacy CANDU-6 2D cell is discussed. Numerical results have been confronted to those of continuous-energy Monte Carlo and Collision Probability methods, establishing very good level of accuracy of the Probability Table Monte Carlo method.

1. Introduction

Given the constant growth in term of computational power of modern computers, the Monte Carlo method is becoming a feasible alternative for production calculations. In particular, traditionally lattice calculation of group constants can possibly be done with a Monte Carlo method, provided that its calculation time remains acceptable compared to legacy CP/MoC cell codes.

A preliminary work done by B. Arsenault [1,2] has set the basis of a Monte Carlo module in the lattice code DRAGON [3]. The primary objective was to implement 2D/3D Monte Carlo capabilities within DRAGON, in such a way that a considerable part of the existing modules can be adequately reused. Such a tool can then be applied to the evaluation of macroscopic cross-sections of any type of reactors, in addition to the 2D/3D deterministic methods such as Pij or MoC. In its first implementation, the Monte Carlo code can handle only macroscopic cross-sections, coming from a preliminary deterministic group constants generation. Our first work was to enable the use of microscopic, multi-group cross-sections as input library. An innovative aspect of the Monte Carlo module was the new capability to use probability table cross-sections, already available in DRAGON for advanced self-shielding models. The purpose is twofold: at a first step, Monte Carlo calculations based on probability table cross-sections are much faster than continuous-energy ones. Second, we can reuse the library processing done in the LIB: module of DRAGON, in charge of the generation of the internal library of cross-sections and of the probability tables cross-sections.

Motivations for developing such a tool are various. We can by now propose a Monte Carlo alternative to classical deterministic schemes with the same geometrical inputs and library

databases. Such a redundancy can be very useful for assessing the performance of the code. For instance, the performance of self-shielding methods can be directly evaluated.

This paper is divided in three parts. First, we briefly introduce the probability table method, useful for representing resonant cross-sections. Then, a description of the Monte Carlo module of DRAGON is given. Finally, a comparative study of a regular CANDU-6 cell is detailed, using the continuous-energy Monte Carlo reactor physics code SERPENT [4], the DRAGON Collision Probability method with the NXT: tracking operator, and our new probability table Monte Carlo module.

2. Probability table cross sections

2.1 Historical overview

Levitt [5] and Cullen [6] in the USA, and independently Nikolaev [7] in Russia have proposed the probability table representation of cross sections in order to improve the accuracy of neutron transport calculations. In this formalism, the cross-sections are replaced by their probability densities, which are then discretized in quadrature sets called probability tables. For a given energy range, a set of discrete values of cross-sections is derived, each of them associated with a weight. Different varieties of probability tables for cross sections have been so far introduced, depending on the way they are computed. In continuous-energy Monte Carlo codes, probability table (PT) cross sections generated by the PURR module of NJOY [8] are intensively used in the unresolved range. It is also possible to derive probability tables for cross-sections in the whole energy spectrum. PT cross sections can be then used to perform transport calculation by either Monte Carlo or deterministic methods. For instance, the LLNL code TART [9] runs Monte Carlo neutron transport calculations with PT cross-sections in the whole energy range. It is important to clarify a point of terminology here: any transport equation in which cross-sections are replaced by probability densities leads to the sub-group or multiband method. A traditional field of application of the subgroup method is for self-shielding correction of resonant cross-sections, mandatory when multigroup cross-sections are employed [10]. When a multigroup library is generated by NJOY, a flux weighting of the cross-sections is carried using a flux typical of the reactor spectrum (e.g. Maxwellian, 1/E, fission). However, this approach fails for resonant isotopes. Generally, a two-step scheme is employed at the cell-level calculation: a self-shielding stage is first realized, leading to effective cross-sections. These effective cross-sections are then used in the main flux calculation.

The use of probability tables in the whole spectrum can be seen as an extension of the multigroup approximation. In the particular case of the Monte Carlo transport method, the switch of a multigroup algorithm over a sub-group one is quite straightforward. In a resonant group, the discrete value of the cross-section will be sampled directly among the base points of the probability table. The self-shielding effect is directly taken into account, in such a way that preliminary calculations of effective cross-sections are no more required. For a non-resonant group, the unique probability table base point will merely coincide with the multigroup cross-section, with an associated weight set to one.

2.2 Mathematical definition

The mathematical definition of probability table differs in the literature. Levitt defines the probability tables as quadrature sets where the point bases are set a priori. In their relative works, Nikolaev and Cullen define a quadrature set where point bases and weights are simultaneously computed. The CALENDF method [10] is an outgrowth of this last formalism, and let to the definition of mathematical, moment-based probability tables. In this case, cross-sections are represented using probability densities, which are then discretized in quadrature called probability tables. Moment-based probability tables are commonly used in different self-shielding methods, for instance in the APOLLO2 lattice code [11], the ECCO fast reactor lattice code [12], or in the DRAGON lattice code for different subgroup methods detailed in Refs. [9], [13] and [14]. We retained the CALENDF formalism for its mathematical consistency: weights are positives, and base points are included in the support $[\min(\sigma(u)),\max(\sigma(u))]$.

It is also possible to compute correlated probability tables with this formalism. Indeed, probability tables suffer from an approximation that could be compared to the *statistical hypothesis* made in self-shielding models. As a result, they are best suited for the upper part of the resonant domain, where correlated effects vanish. A detailed overview of the method for computing mathematical probability tables can be found in Refs. [11] and [13].

The direct use of probability table cross-sections in the whole energy range require to take into account two different correlations. In the lower part of the resolved domain, the slowing-down kernel is acting over a range that is not long compared to the average neutron lethargy, and correlations can occur between different energy groups. A simple technique to overcome slowing-down correlated effects consists in refining the energy mesh in the resolved energy range. This has been done in Refs. [14] and [15], where the SHEM 281 group structure has been extended to 295 and 361 groups. Also, correlations occur in case of overlapping resonances for two different isotopes or for the same isotope present at different temperatures in the system. This phenomenon is known as *mutual* self-shielding and can be added up by defining correlated weights between two isotopes, leading to the definition of 2D probability tables table cross-sections. A probability density $\Pi(\sigma)$ can be defined from the microscopic total cross section $\sigma(u)$ as depicted in Fig. 1.

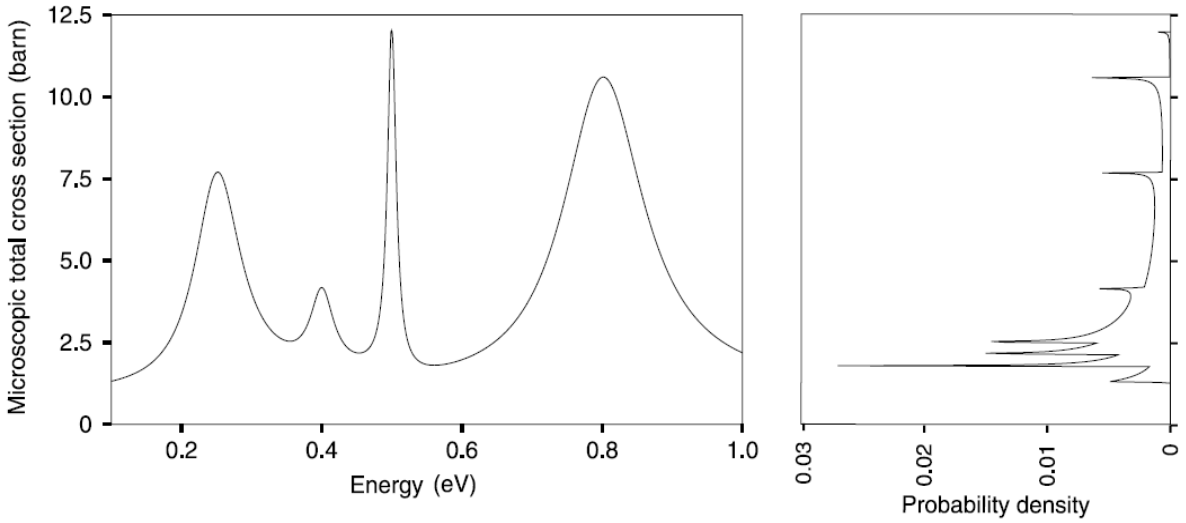

Figure 1: cross-section density probability

We define $\Pi(\sigma)d\sigma$ as the probability for the microscopic cross-section to have its value between σ and $\sigma+d\sigma$.
Then, any Riemann integral in lethargy with a σ-dependent integrand can be replaced by its Lebesgue equivalent integral:

$$\frac{1}{\Delta u_g}\int_{u_{g-1}}^{u_g} du f(\sigma(u)) = \int_0^{\max(\sigma)} d\sigma \Pi(\sigma) f(\sigma) \tag{1}$$

with $\Delta u_g = u_g - u_{g-1}$. The probability density $\Pi(\sigma)$ is next expanded in a series of K Dirac distributions, centered at the discrete values σ_k of the microscopic cross-sections. Each discrete level k will be called a *subgroup* and will be characterized by a weight ω_k:

$$\Pi(\sigma) \approx \sum_{k=1}^{K} \omega_k \delta(\sigma - \sigma_k) \tag{2}$$

with $\sum_{k=1}^{K} \omega_k = 1.$
The probability table can then be written as

$$\frac{1}{\Delta u_g}\int_{u_{g-1}}^{u_g} du f(\sigma(u)) \approx \sum_{k=1}^{K} \omega_k f(\sigma_k). \tag{3}$$

In the remaining of this paper, a 1D probability table of order L for a given isotope in an arbitrary group g for a reaction ρ will correspond to a mathematical expression of the form $\{\omega_k, \sigma_{\rho,k}\}_{k\in[1,L]}$.

2.2.1 2D probability table cross-sections

We also define correlated probability tables between pair of resonant isotopes. A conditional probability density $\Pi(\sigma^a, \sigma^b)$ is introduced in such a way that $\Pi(\sigma^a, \sigma^b)d\sigma^a d\sigma^b$ represents the

probability of isotope a to have its microscopic total cross-section between σ^a and $\sigma^a + d\sigma^a$ when isotope b have its microscopic cross-section between σ^b and $\sigma^b + d\sigma^b$. Using the same property as before, any Riemann integral in lethargy with a σ^a and σ^b integrand can be replaced by an equivalent Lebesgue integral:

$$\frac{1}{\Delta u_g}\int_{u_{g-1}}^{u_g} du f\left[\sigma^a(u),\sigma^b(u)\right] = \int_0^{\max(\sigma^a)} d\sigma^a \int_0^{\max(\sigma^b)} d\sigma^b \Pi(\sigma^a,\sigma^b) f(\sigma^a,\sigma^b) \tag{4}$$

The probability density is then replaced by a sum of Dirac distributions:

$$\Pi(\sigma^a,\sigma^b) = \sum_{k=1}^{K}\sum_{l=1}^{L} \omega_{k,l}^{a,b}\delta(\sigma^a - \sigma_k^a)\delta(\sigma^b - \sigma_l^b) \tag{5}$$

Combining Eqs. [4] and [5] leads to the following discretization

$$\frac{1}{\Delta u_g}\int_{u_{g-1}}^{u_g} du f\left[\sigma^a(u),\sigma^b(u)\right] = \sum_{k=1}^{K}\sum_{l=1}^{L} \omega_{k,l}^{a,b}\delta(\sigma^a - \sigma_k^a)\delta(\sigma^b - \sigma_l^b) f(\sigma_k^a,\sigma_l^b) \tag{6}$$

where the correlated weight matrix is normalized in such a way that

$$\sum_{k=1}^{K} \omega_{k,l}^{a,b} = \omega_l^b \text{ and } \sum_{l=1}^{L} \omega_{k,l}^{a,b} = \omega_k^a \tag{7}$$

In this case, 2D probability tables between correlated isotopes a and b can be used to sample the point base cross-sections of isotope a given those of the isotope b. Mathematically, this property can be written as a conditional probability of having the point base cross-section in subgroup k for isotope a, given that isotope b has its point base cross-section in subgroup l:

$$P(\sigma^a = \sigma_k^a \mid \sigma^b = \sigma_l^b) = \frac{\omega_{k,l}^{a,b}}{\omega_l^b} \tag{8}$$

Note also that if correlations vanish, $\omega_{k,l}^{a,b} = \omega_k^a \omega_l^b$ and 2D probability tables are simply 1D ones.

3. Monte Carlo random walk with probability tables in the DRAGON lattice code

A Monte Carlo algorithm using the Woodcock delta-tracking method [1] was already available in the DRAGON lattice code, restricted to multigroup cross-sections. Modifications have been undertaken to use probability table cross-sections. A simplified overview of the random walk is given below.

1. Set the properties of the source neutron:
   - Spatial co-ordinates.
   - Index of the fissile isotope *i* producing the neutron.
2. Sampling the energy group in $\chi_i(E)$.
3. Sampling the initial direction.
4. Sampling of the subgroup index in the probability table:
   - In case of 1D probability table: sampling for each isotope *i* the microscopic total cross-section $\sigma_t^i = \sigma_{t,k}^i$ with a probability ω_k. Note that all cross-sections for partial reactions come along, with a given value of $\sigma_\rho^i = \sigma_{\rho,k}^i$.
   - In case of correlations between 2 isotopes *a* and *b*: sampling for each isotope the microscopic total cross-section $\sigma_t^b = \sigma_{t,l}^b$ with a probability of $\frac{\omega_{k,l}^{a,b}}{\omega_l^b}$, *b* generally set as the fissile isotope producing the neutron. Correlated isotopes are

determined during the processing: e.g., they are resonant isotopes in the same mixture.

5. Calculation of total cross-sections in group *g* for each mixtures containing *i* isotopes, $\Sigma_{t,r,g} = \sum_{i\in[r,g]} N_i \sigma_t^i$ where N_i is the isotopic density of isotope *i*.
6. Determination of the majorant cross-section in total volume $\Sigma_{m,g} = \max_{r\in V}(\Sigma_{t,r,g})$.
7. Sampling the free path using the majorant cross-section,
8. Sampling if the collision is real or virtual:
   - In case of virtual collision, new sampling of the free path with the same direction
   - In case of real collision
     - Sampling of the collided isotope *i* in region $\{r,g\}$ with a probability of $\frac{N_i\sigma_i}{\Sigma_{t,r,g}}$.
     - Sampling the reaction using $\frac{\sigma_\rho^i}{\sigma_t^i}$.
     - In case of scattering, the secondary group is set using isotropic scattering cross-sections, and the history continues. (n,xn) reactions are for the time being considered as scattering reactions, the weights of the neutrons are then consistently increased.
     - If fission occurs, the index of the isotope is stored and the history is terminated.
     - In case of absorption, the history is terminated.

The Monte Carlo algorithm proposed above is currently implemented as an independent module called MC:, in a developing version of the lattice code DRAGON. The flowchart of a Monte Carlo calculation in DRAGON is displayed in Fig. 2.

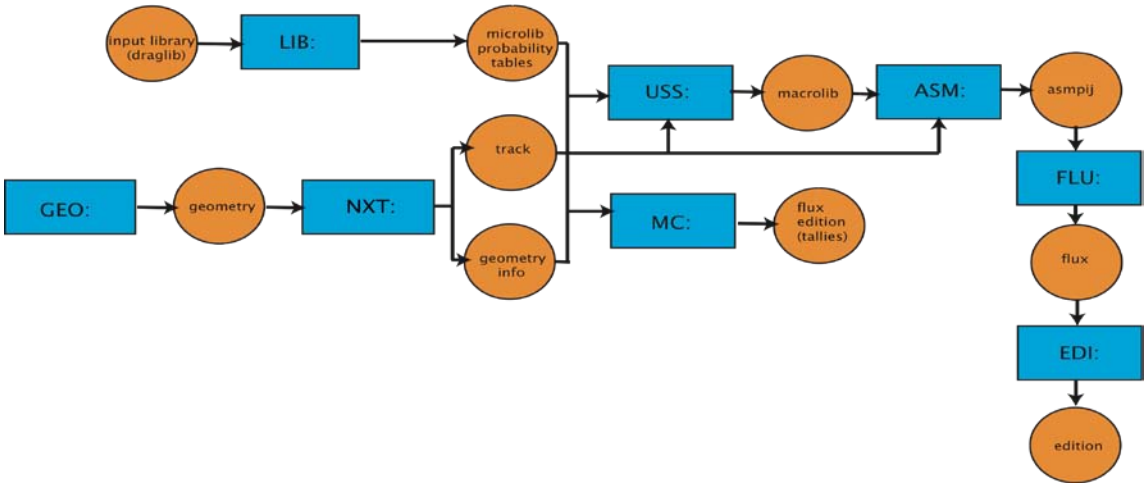

Figure 2: flowchart of DRAGON MC and CP calculation

4. Study of a CANDU lattice cell

A typical CANDU6 lattice cell has been retained here for illustrating the performance of our method. We selected a 2D Cartesian cell with a lattice pitch of 28.56 cm, constituted of 37 cylindrical fuel pin cells with heavy water as coolant, surrounded by pressure tubes, helium gap, calandria tubes and finally heavy water as moderator.

Geometrical inputs are displayed respectively for DRAGON CP method and Monte Carlo (both DRAGON MC and SERPENT) in Figs. 3 and 4.

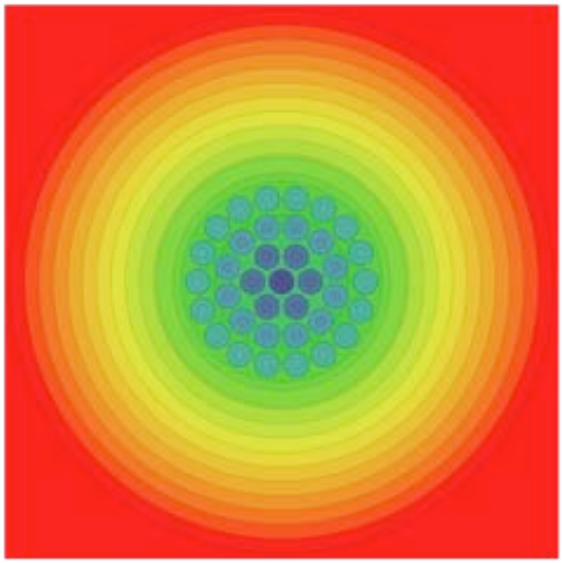

Figure 3: CP input geometry

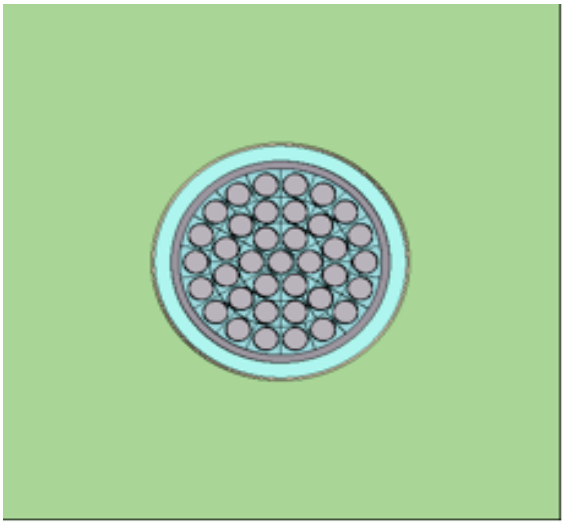

Figure 4: MC input geometry

The study done here is a classical evaluation of the coolant void reactivity (CVR). Two fundamental mode calculations are done without leakage, using periodic conditions at the boundaries. The first one uses the regular CANDU-6 cell modeling, while in the second one the coolant is removed from the pressure tube. The CVR will be then evaluated using

$$\rho_{CVR} = \left(\frac{1}{k_{eff}^{full}} - \frac{1}{k_{eff}^{voided}} \right) \tag{9}$$

Three sets of results will be confronted, using:

- DRAGON CP: collision probability method.
- DRAGON MC: Monte Carlo method with probability table cross sections.
- SERPENT: Monte Carlo method with continuous-energy cross-sections.

As the two simulations are independents, standard deviations coming along Monte Carlo k_∞ estimators are propagated using

$$\sigma_{cvr} = \sqrt{\frac{(\sigma^{voided})^2}{(k_{eff}^{full})^4} + \frac{(\sigma^{full})^2}{(k_{eff}^{voided})^4}} \tag{10}$$

For both DRAGON simulations, the input cross-sections library is a JEFF3.1, SHEM-361 groups in the Draglib format [16]. For the SERPENT code, a JEFF3.1 input library in the ACE format has been chosen. As the options and the version of NJOY99 differed slightly between the Draglib and the ACE libraries processing, we expect to get some discrepancies between both codes. However, the consistency is ensured between DRAGON CP and MC methods. In this case, probability tables are used between 22.5 eV and 1.23×10^5 eV for the following resonant isotopes: Zr91, U235 and U238. A transport correction to the total and scattering cross-sections, computed in DRAGON during the LIB: processing, can also be applied to take into account anisotropic scattering in the multigroup cross-sections for DRAGON MC and CP methods.

4.1 Deterministic lattice calculation options

Any standard cell calculation in DRAGON implies at least two steps. The first one consists in performing a self-shielding correction of the cross-sections, typically with a simplified geometrical model. In our case, we have chosen a sub-group method as implemented in the module USS: of DRAGON, with exactly the same probability tables that in the Monte Carlo module. The retained self-shielding algorithm is detailed in Ref. [14], and is known as the Subgroup Projected Method. In our case, we have slightly modified the primary approach of this formalism by replacing the Root Mean Square (RMS) computed base points of the scattering and fission cross-sections by a pure CALENDF method. Indeed, these CALENDF probability tables have been established as mandatory for the Monte Carlo module. We therefore enhance consistency of both calculations, enabling us to confront in detail the performance of the self-shielding stage; or inversely, of the Monte Carlo calculation. No discretization of the moderator is performed in the self-shielding stage, and a track density of 50 tracks/cm^{-1} with an azimuthal quadrature order of 12 angles in $[0, \frac{\pi}{2}]$ are set in the NXT: tracking operator. Results have been established poorly sensitive to these parameters. Regarding the main flux calculation, the same

tracking options are used, with this time a six and a ten rings' discretization of the coolant and the moderator respectively, and two rings for the fuel cells, as illustrated in Fig. 3.

4.2 Monte Carlo options

The options used in both SERPENT and DRAGON MC: module are the same: 500 active cycles of 3000 neutrons, with 50 discarded cycles. The k_∞ and reaction rates are given by the virtual collision estimator, due to the fact that both code use a delta-scattering rejection technique for the tracking. As correlation effects between isotopes are considered negligible in this case, only 1D probability tables are computed.

4.3 Numerical results

4.3.1 CVR of a CANDU-6 2D cell

The infinite multiplication factor k_∞ is displayed in Tab. 1 for each case (full cell and voided cell), associated with the absolute difference between the Pointwise Monte Carlo results: $\delta k_\infty = k_\infty^{dragon} - k_\infty^{serpent}$, in pcm ($10^{-5}$).

Table 1: k_∞ for a CANDU-6 cell

	DRAGON (CP)		DRAGON (MC)		SERPENT
Case	k_∞	δk_∞ with Serpent	$k_\infty \pm \sigma$	δk_∞ with Serpent	$k_\infty \pm \sigma$
Full cell	0.93442	299 pcm	0.93579 +/- 30 pcm	437 pcm	0.93142 +/- 30 pcm
Voided cell	0.95480	236 pcm	0.95513 +/- 30 pcm	269 pcm	0.95244 +/- 30 pcm

CVR are also computed in Tab. 2.

Table 2: ρ_{CVR} for a CANDU-6 cell

$\rho_{CVR}^{SERPENT}$	2368 +/- 5 pcm
$\rho_{CVR}^{DRAGON(MC)}$	2163 +/- 5 pcm
$\rho_{CVR}^{DRAGON(CP)}$	2285 pcm

We observe that probability table Monte Carlo k_∞ and ρ_{CVR} are consistent with those obtained by the legacy collision probability method and to the punctual Monte Carlo code SERPENT. Note also that the difference between CP and MC methods in DRAGON is in general below 100 pcm for both k_∞ and ρ_{CVR}.

4.3.2 Reactions rates and spectrum

In this section, we compare reaction rates generated with the MC: module of DRAGON toward CP and SERPENT ones on the CANDU-6 cell with coolant. A complete homogenization is carried on the whole geometry, with an energy condensation to four groups $\{g_1, g_2, g_3, g_4\}$ defined in Tab. 3.

Table 3: energy range for group condensation

Group	Energy range (eV)
1	] 5.10E6 15E6 [
2	] 5.10E3 5.10E6 [
3	] 0.625 5.10E3 [
4	] 5E-4 0.625 [

Table 4: relative difference on reaction rates

Reaction type	Relative difference with DRAGON-CP (%)	Relative difference with SERPENT (%)
Fission g1	0.931	3.931
Fission g2	2.078	1.724
Fission g3	-0.471	-0.340
Fission g4	0.112	0.577
Absorption g1	0.337	-9.74
Absorption g2	0.071	-0.628
Absorption g3	1.662	1.892
Absorption g4	0.131	0.393

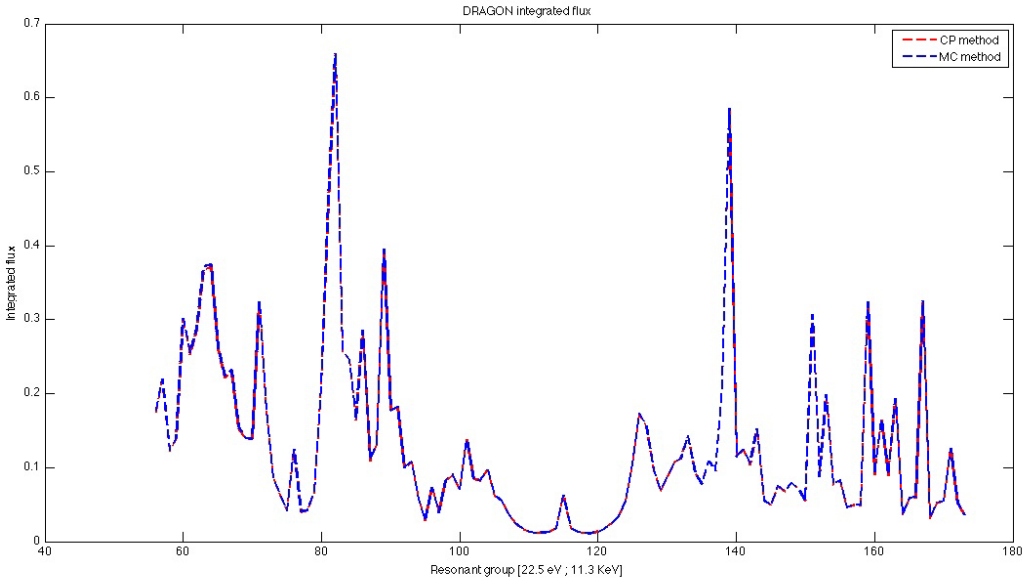

Figure 4: integrated flux for CP and MC method in DRAGON in resonant groups

The relative differences between both DRAGON and SERPENT reaction rates are generally below a few percent. We also note that the integrated flux spectrum is equivalent for MC and CP methods on a CANDU-6 cell.

5. Conclusion

We have developed an independent Monte Carlo method in the lattice code DRAGON, available in a module named MC:. This module has been recently rewritten in a FORTRAN 2003 standard, and should be released within the DRAGON version 5. Validation using 2D PWR and CANDU pin cells has established good characteristics of this new solver. Further work will be undertaken to check consistency of assembly-level calculations. Validation against selected criticality-safety benchmarks, ACR, Pressurized Water Reactor and fast breeder reactor cells will be undertaken. We are currently implementing legacy methods permitting the treatment of anisotropic scattering reactions in Monte Carlo multigroup calculation, such as the Discrete Angle Technique. Validation of these models will terminate the Ph.D. work. At a longer time scale, the introduction of a leakage model in the Monte Carlo method and the coupling of module MC: with the depletion solver EVO: of DRAGON are required steps before considering pure Monte Carlo lattice calculations in DRAGON5.

6. References

[1] B. Arsenault, R. Le Tellier, A. Hebert, "Efficiency of the Delta-Tracking technique for Monte Carlo Calculations Applied to Neutron Transport Simulations of the Advanced CANDU Reactor Design", Interlaken, Switzerland, PHYSOR 2008, September 14-19 2008.

[2] Hébert, A., “Applied Reactor Physics”, Presses Internationales Polytechnique, Montréal, 2009.

[3] Marleau, G., Hébert, A. and Roy, R., “New Computational Methods Used in the Lattice Code Dragon”, Proc. Int. Top. Mtg. On Advances in Reactor Physics, Charleston, USA, March 8-11, 1992. Dragon Version4 and cross-section libraries can be downloaded from the web site at http://www.polymtl.ca/nucleaire/.

[4] Leppänen, J., “PSG2 / Serpent: a Continuous-energy Monte Carlo Reactor Physics Burnup Calculation Code”, Methodology, User's manual, Validation report, 2009.

[5] Levitt, L.B, “The Probability Table Method for Treating Unresolved Neutron Resonances in Monte Carlo Calculations”, *Nuclear Science and Engineering*, **54**, 450, 1972.

[6] Cullen, D.E., “Application of the Probability Table Method to Multigroup Calculations of Neutron Transport”, *Nuclear Science and Engineering*, **55**, 387--400, 1974.

[7] Nikolaev, M. N. “Comments on the Probability Table Method”, *Nuclear Science and Engineering*, **61**, 286, 1976.

[8] MacFarlane, R. E. and Muir, D. W., “NJOY99.0 Code System for Producing Pointwise and Multigroup Neutron and Photon Cross Sections from ENDF/B Data”, Los Alamos National Laboratory, PSR-480/NJOY99.0, 2000.

[9] Cullen, D.E., "TART2005: A Coupled Neutron-Photon 3-D, Combinatorial Geometry, Time Dependent Monte Carlo Transport Code", Lawrence Livermore National Laboratory, UCRL-SM-218009, 2005.

[10] Ribon, P. and Maillard, J.M, "Les tables de probabilité. Application au traitement des sections efficaces pour la neutronique", Commissariat à l'Energie Atomique, CEA-N-2485, 1986.

[11] Hébert, A. and Coste, M., "Probability Tables for Self-Shielding Calculations in Lattice Codes", *Nuclear Science and Engineering*, **142**, 245-257, 2002.

[12] Grimstone, M.J., Tullett, J.D., Rimpault, G., "Accurate Treatments of Fast Reactor Fuel Assembly Heterogeneity with the ECCO Cell Code", Proc. Int. Conf. Physics of Reactors: Operation, Design and Computation: PHYSOR 90, Marseille, France, April 23–27, 1990.

[13] Hébert, A., "The Ribon Extended Self-Shielding Model", *Nuclear Science and Engineering*, **151**, 1--24, 2005.

[14] Hébert, A., "Development of the Subgroup Projection Method for Resonance Self-Shielding Calculations", *Nuclear Science and Engineering*, **162,** 56--75, 2009.

[15] Hébert, A. and Santamarina, A., "Refinement of the Santamarina-Hfaiedh energy mesh between 22.5 eV and 11.4 KeV", Proc. Int. Conf. On the physics of reactors. Nuclear Power: A Sustainable Resource, PHYSOR 2008, Interlaken, Switzerland, 2008.

[16] Hébert, A., Saygin, H., "Development of DRAGR for the Formatting of DRAGON Cross-Section Libraries", Seminar on NJOY-91 and THEMIS for the Processing of Evaluated Nuclear Data Files, Saclay, France, April 7–8, 1992.